OPTICAL PROPERTIES OF CIRCUMSTELLAR SILICATE GRAINS*, **

KYUNG-WON SUH***

Department of Astronomy and Meteorology, Yonsei University, Seoul, Korea

(Received 24 August, 1990)

Abstract. The optical properties of circumstellar silicate dust grains around oxygen-rich giant stars are investigated with close attention to infrared observations of OH/IR stars. The optical constants are deduced from available astronomical and laboratory data. The deduced opacities at longer wavelengths ($\lambda \geq 12$ μm) for OH/IR stars are higher than the one for M-type Miras possibly because of the change of optical constants depending on temperature of dust grains. Absorption and scattering efficiencies are evaluated for various grain size distributions and shapes. The results of detailed radiative transfer model calculations based on our dust parameters are compared with observational data. The Planck mean values incorporating substantial far-infrared absorption are also calculated.

1. Introduction

Infrared observations of M-type Miras and OH/IR stars suggest the presence of silicate dust grains in the outer shells around them. The typically show 9.7 μm and 18 μm silicate features. The M-type Miras show emitting 9.7 μm and 18 μm features, while OH/IR stars which have thicker dust shells show absorbing features at the same wavelengths (e.g., Engels *et al.*, 1983). The 9.7 μm feature is interpreted as stretching vibrations of the Si–O bond (Woolf and Ney, 1969) while the 18 μm feature is interpreted as bending vibration of the bond angle in O–Si–O group (Treffers and Cohen, 1974). But the chemical composition and structure of the condensate are not well known since the two features only refer to a special active group which is present in many different materials.

Using mainly the classical nucleation theory, dust formation processes are investigated, in a steady state (e.g., Yamamoto and Hasegawa, 1977) and in the expanding gas flow (Deguchi, 1980; Kozasa *et al.*, 1984; Papoular and Prégourié, 1986; Suh, 1988). Given the fundamental stellar parameters and a constant mass loss rate, the theory yields the grain size and grain formation time-scale as well as the dust and gas densities and velocities.

A number of authors have investigated the optical properties of silicate dust grains (Jones and Merrill, 1976; Draine and Lee, 1984; Prégourié and Papoular, 1985; Bedijin, 1987; Volk and Kwok, 1988) with various assumptions on input parameters and degrees of sophistication. The opacity pattern appears to be different for Miras and OH/IR stars with the same other input parameters as Bedijin (1987) and Volk and Kwok (1988) mentioned. We may have to assign different opacity pattern for each object. But there

* Yonsei University Observatory Contribution No. 91.

** Department of Astronomy and Space Science, Chungbuk National University Contribution No. 4.

*** Present address: Dept. of Astronomy and Space Science, Chungbuk National University, Cheongju-City, Korea.

Astrophysics and Space Science **181**: 237–250, 1991.

is a tendency which suggests that the difference is due to the different amount of cold dust grains. In this work we have deduced the best-fitting opacity pattern and optical constants for extreme 2 cases: M-type Miras and OH/IR stars. They are obtained from laboratory and observational data after detailed radiative transfer model calculations. Keeping in mind the results of stellar wind models and pulsation-shock models, we suggest a model parameter for the structure of the dust shells.

Our work is different from recent previous work in the following aspects. The present work is to concentrate on optical properties, so our radiative transfer calculations are much more accurate than Bedijin's (1987); the scattering is considered, 70 wavelength and 125 radial grid points are used. Using finer wavelength grid points suggests the better and more reliable comparison with observations. In comparing our models with observations, we concentrate on some well observed objects to test the fitting in detail.

2. Optical Constants, Efficiencies

One way to find the relevant sets of optical constants for circumstellar dust grains is to solve the radiative transfer problem for typical models and compare with observations when we know the appropriate stellar and dust shell characteristics. After many trials, we have found a good opacity pattern which fits better with observations, but does not stray too far from the known characteristics of silicate materials. In this section we discuss the optical properties based on optical constants deduced from model fitting. We will discuss the results of model calculations in the next section.

The optical depth can be expressed as $\tau_\lambda = \int \alpha_\lambda \, dz$, where the extinction coefficient α_λ is $\alpha_\lambda = N_g Q_{\text{ext}\,\lambda} \pi a^2$, where N_g is number density of dust grain; a, the radius of grain. Q_{ext} is the extinction efficiency factor which has two terms: $Q_{\text{ext}} = Q_{\text{sca}} + Q_{\text{abs}}$, where Q_{sca} is the efficiency factor for scattering and Q_{abs} is the efficiency factor for absorption. The radiation pressure efficiency factor Q_{pr} is defined as $Q_{pr} = Q_{\text{ext}} - GQ_{\text{sca}}$, where $G = \langle \cos\theta \rangle$ is the anisotropy factor and θ is the angle between the incident wave and the scattered wave.

TABLE I

$\tau_{\text{ext},\lambda}/\tau_{\text{ext},9.7\,\mu\text{m}}$ (albedo) for astronomical silicate

λ	Suh (this paper)	Volk and Kwok (1988)	Draine and Lee (1984)	Jones and Merrill (1976)
1	2 (0.17)	1.5	0.85 (0.62)	2 (0.21)
5	0.13	0.27	0.08	0.273
7	0.1	0.2	0.08	0.22
12	0.17	0.3	0.43	0.25
18	0.5 [0.7][a]	0.5	0.36	0.5
27.5	0.174 [0.273][a]	0.21	0.16	0.466
40	0.075 [0.122][a]	0.13	0.076	0.0726
100	0.01 [0.02][a]	0.04	0.01	0.0034

[a] For absorbing features (OH/IR stars).

For given characteristics of the dust material, namely optical constants at given wavelength and the size or size distribution of the grains, optical efficiency factors are calculated by using the Mie theory. We have used a computer subroutine program which has been developed by Bohren and Huffman (1983) and modified by us to include the anisotropy factor (G) which is useful for calculating radiation pressure efficiency factors.

After comparing our model calculations with observations, we have made the opacity patterns which fits observations well. The opacity pattern we find for M-type Miras (which show emitting features) is similar to that of previous work (Jones and Merrill, 1976; Volk and Kwok, 1988); this fits observations of Miras fairly well. But for OH/IR stars which show absorbing features we have significantly modified the opacity pattern;

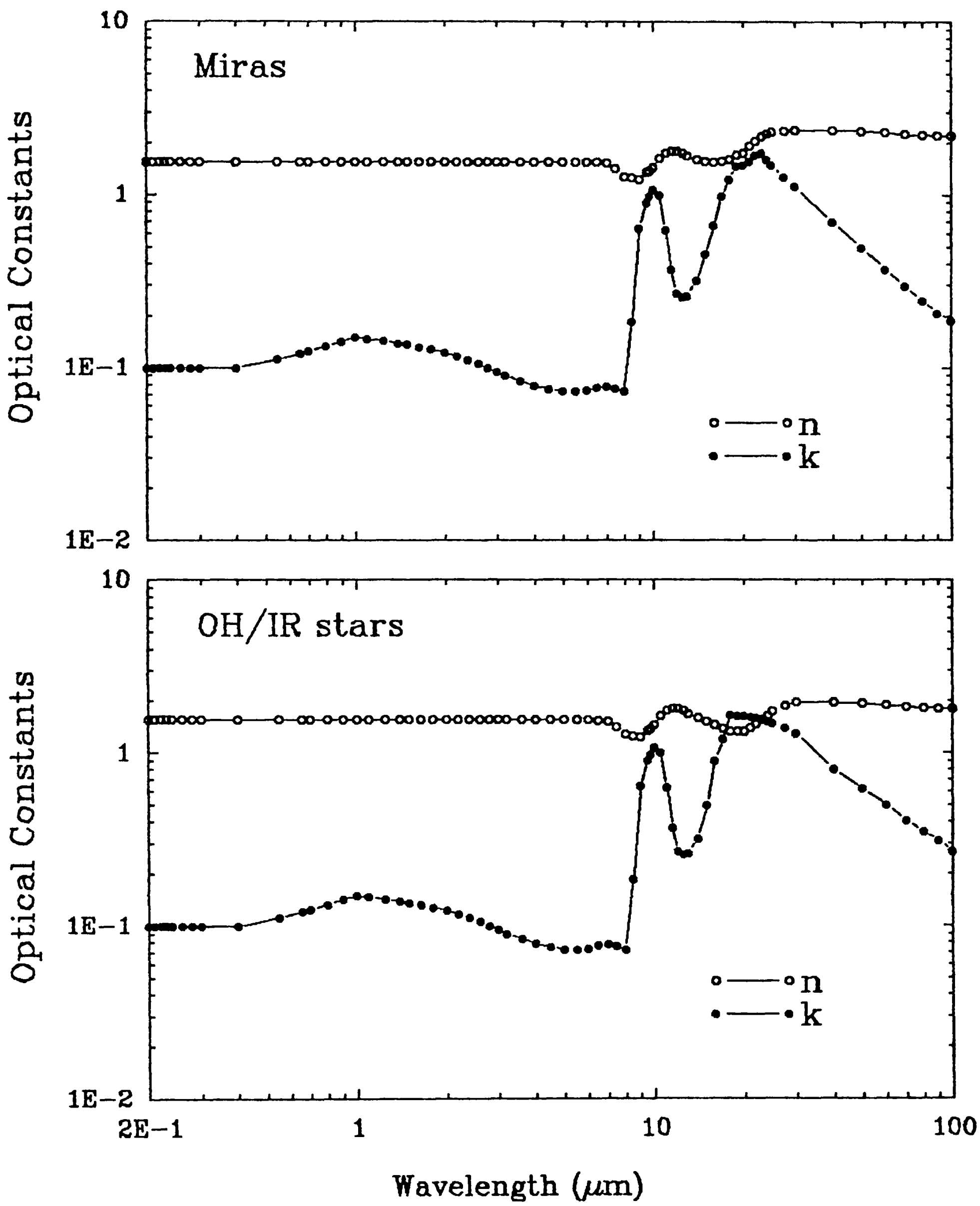

Fig. 1. Optical constants of silicate dust grains deduced for M-type Miras and OH/IR stars.

we need higher opacities at longer wavelengths ($\lambda \geq 12$ μm) to reproduce the observational data. Table I lists the choices of opacity pattern.

The optical constants (n, k) are parts of index of refraction ($m = n + \mathbf{i} \cdot k$). In the limit of very small grains, the spectral profile of the absorption and extinction efficiencies are independent of grain size but simply related to the imaginary index of refraction k (Prégourié and Papoular, 1985). So we have used laboratory values of n for a typical candidate material Mg_2SiO_4. Day's (1979) values for λ = 8–30 μm and Day's (1981) values for λ = 30–100 μm are used for n, and k is deduced from fitting. For shorter wavelengths, we adopted similar values to those of Draine and Lee (1984) smoothly joined to our values at longer wavelengths.

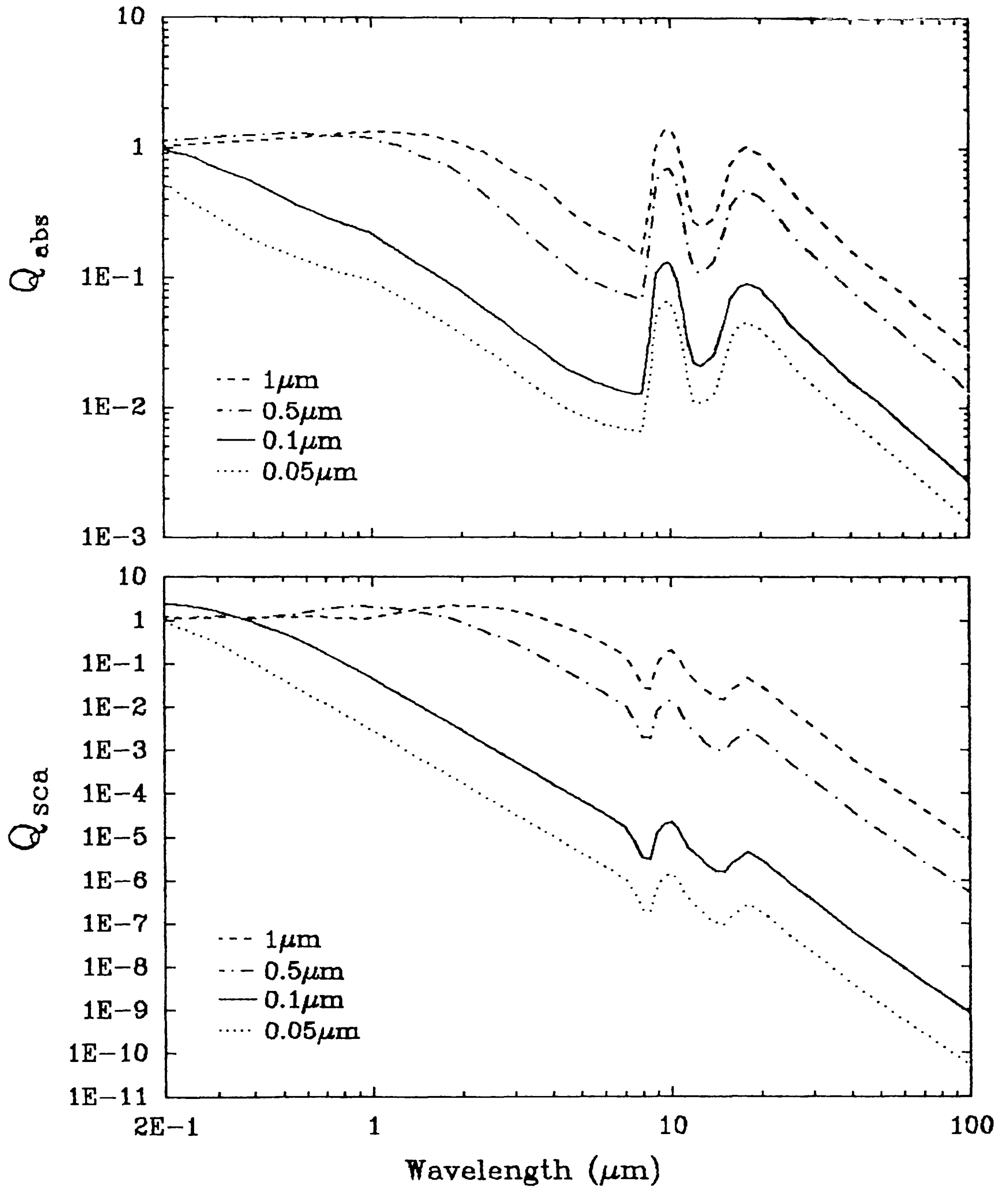

Fig. 2. Absorption and scattering efficiency factors for various spherical grain radius. The optical constants for OH/IR stars are used.

Figure 1 shows the optical constants we deduce for M-type Miras and for OH/IR stars. Figure 2 shows the absorption and scattering efficiency factors for various spherical grain sizes (radii) in the case of OH/IR stars.

The reason why we had to use different opacity pattern for the objects with thicker dust shells (that shows absorbing features) may be found from experiments. Day (1976a, b) found that extinction efficiency is dependent on temperature. The results show that:

Temperature (K)	100	200	400
$Q_{ext}(20\ \mu m)/Q_{ext}(10\ \mu m)$	0.72	0.63	0.5

Namely, when cooled down below about 200 K, the extinction efficiency at 20 μm increases while the extinction at 10 μm remains essentially unchanged. The reason for this change could be due to the change of optical constants depending on the temperature of dust grain. The OH/IR stars have more cold material which contribute to the emergent spectra than Miras, and that could be the reason for having the characteristics at cold temperature. Jones and Merrill (1976) argued that a large optical depth at 9.7 μm in dust colder than about 250 K (or 125 K) is ordinarily required to produce 9.7 μm (or 18 μm) feature significantly in absorption.

Prégourié and Papoular (1986) found the need to have different opacity pattern depending on the location of the contributing dust grains to the emergent spectra and argued that the difference could be due to different grain materials or grain sizes for emitting and absorbing features. But the suggestion of different grain sizes does not appear to contribute the phenomena because different grain sizes do not change $Q_{ext}(20\ \mu m)/Q_{ext}(10\ \mu m)$ even though bigger grains have higher opacity at wider wavelength range.

Figure 3 shows the efficiency factors for spherical and infinite cylindrical silicate grains in the case of OH/IR stars. For absorption, the average values for cylindrical grains does not stray far from that of spherical grains. Our assumption of spherical grains in circumstellar shells is not very unrealistic when we are mainly concerned on absorption at infrared wavelengths.

3. Model Fitting with Observations

Dust grains in the outer shell absorb and scatter the stellar radiation and re-emit it at longer wavelengths. For given characteristics of the central star and the dust shell around it, we may find the emergent spectra by solving the radiative transport problem and compare the results with observation. We may check whether our modeling is accurate or not and find ways to improve our input parameters. We have used Leung's radiative transfer code (Egan *et al.*, 1987). The theory behind this code is explained in Leung (1976). In the present calculations, a radial grid of 125 points and a frequency grid of 70 wavelengths were used.

We have adopted the optical constants as presented in the last section. For grain size,

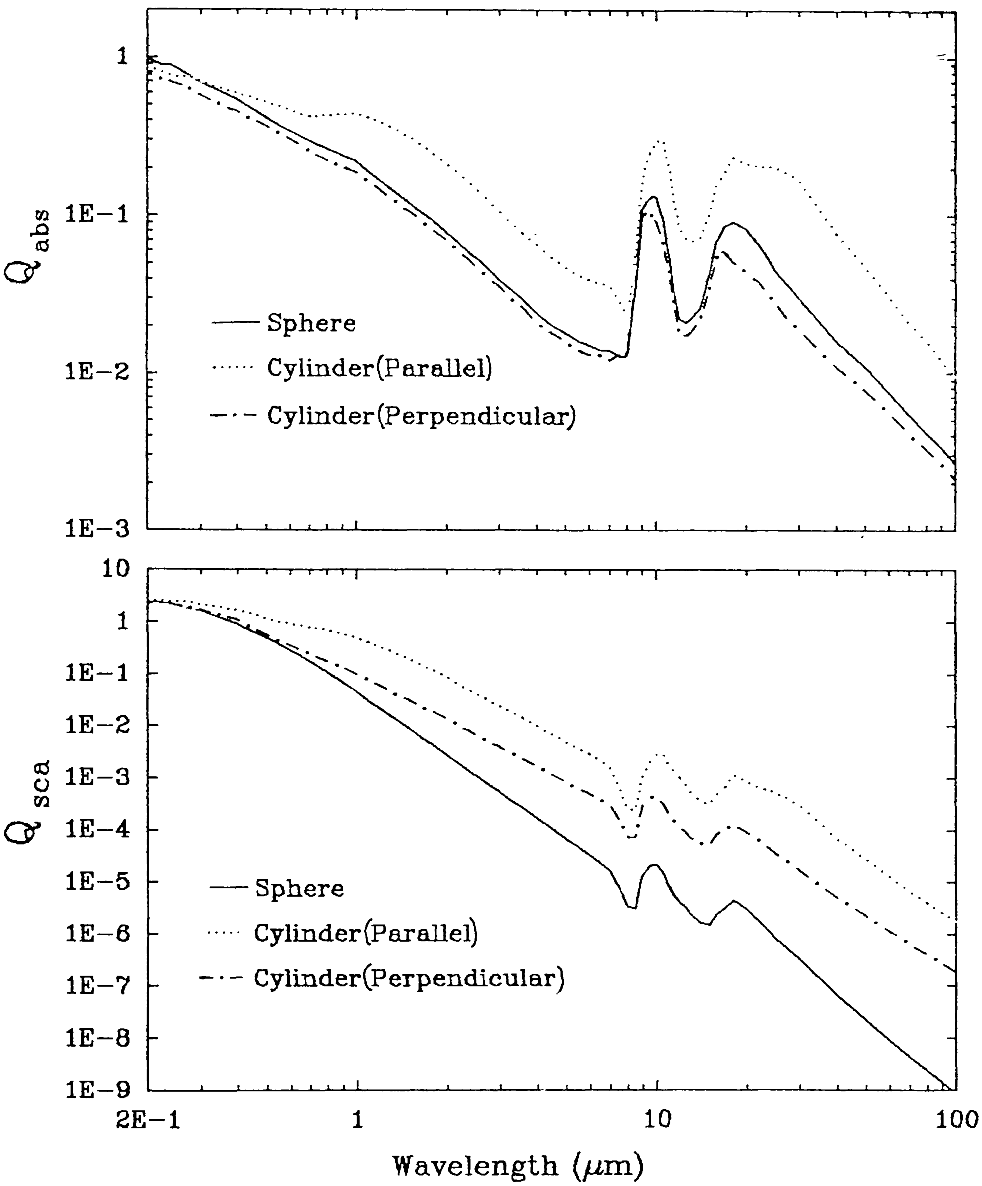

Fig. 3. Absorption and scattering efficiencies for a sphere and an infinite cylinder with the same radius of 0.1 μm. The z-axis of the cylinder is parallel and perpendicular to incident beam. The optical constants for OH/IR stars are used.

a Gaussian distribution with peak radius of 0.1 μm and mean deviation of 0.05 μm has been used. According to classical nucleation theory, the final grain size is calculated to be about 0.1 μm and dust formation and growth time-scale is very short (about a week) compared with other time-scales for typical OH/IR stars' environment (e.g., Suh, 1988). This burst-like grain formation suggests overall constant flow (i.e., the density distribution is $\rho(r) \propto r^{-2}$).

Figure 4 shows the absorption and scattering efficiency factors versus wavelength; this has been used for all of our model calculation for M-type Miras and OH/IR stars. We find that using Gaussian distribution does not make much differences except at

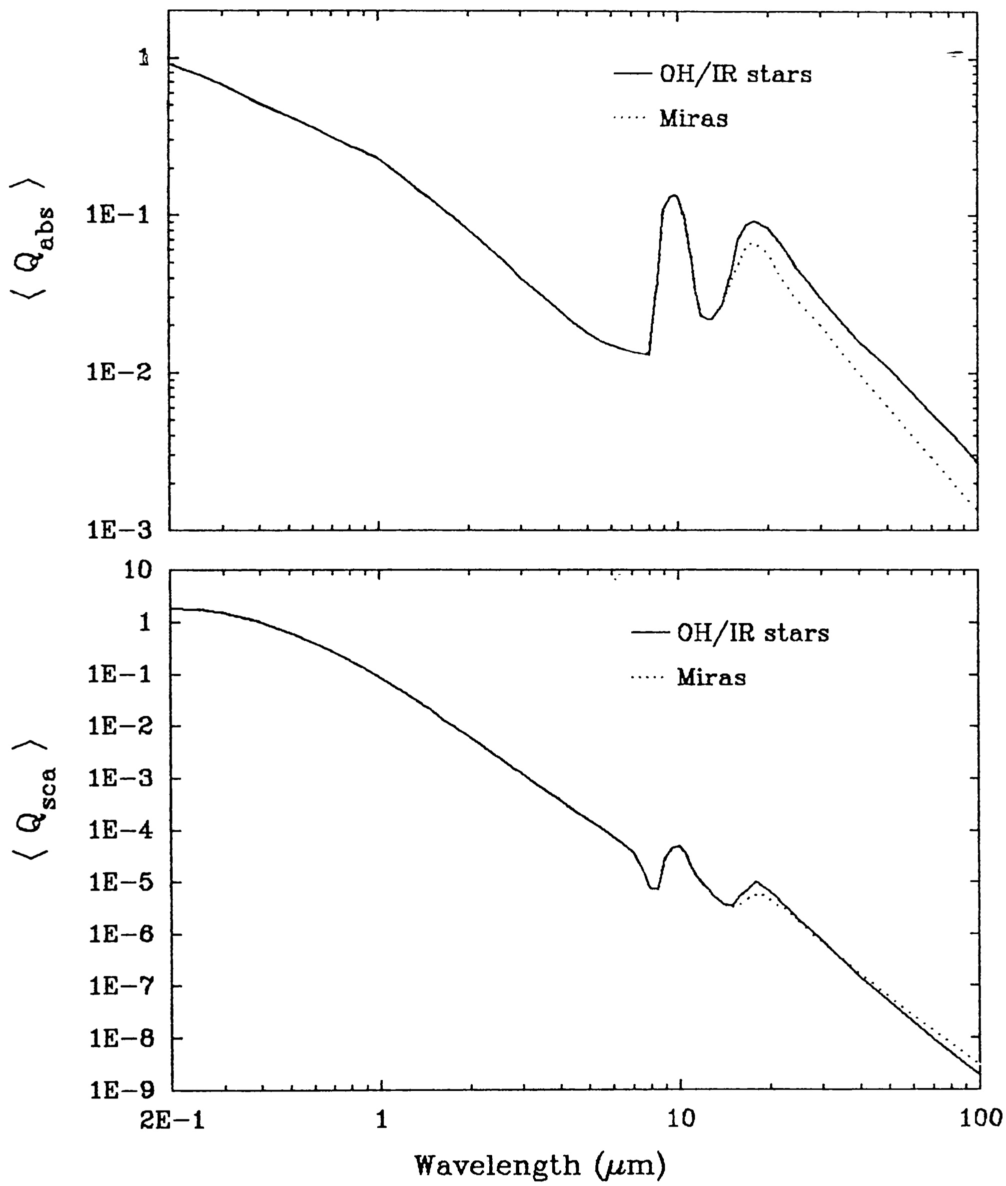

Fig. 4. Absorption and scattering efficiencies for Gaussian size distribution (peak radius = 0.1 μm; mean deviation = 0.05 μm). This is used for the model calculations for M-type Miras and OH/IR stars.

short wavelength ($\lambda \leq 3$ μm) compared with the result for single size. For dust density distributions, we have used a simple power law ($\rho \propto r^{-\beta}$) with βs from 1 to 3. The dust condensation temperature (T_c) is assumed to be 1000 K; dust condensation radius (R_c) is obtained after a few trials. The outer radius of the dust shell is always taken to be 1000 R_c.

Werner *et al.* (1980) argued that a flatter density distribution fits better for dust-thick OH/IR stars with their choice of opacity pattern. Their opacity which is similar to our opacity for Miras was too low at $\lambda \geq 12$ μm to reproduce 18 μm absorption feature (we need $\tau_{9.7\ \mu\mathrm{m}} \geq 40$ to reproduce 18 μm absorption feature with $\beta = 2$!), so smaller β produces more flux at $\lambda > 12$ μm and the 18 μm absorption feature. But we find that the dust density distribution is likely to be $\rho(r) \propto r^{-2}$. With $\beta = 1$ to 1.5 we can reproduce deep 18 μm absorption feature even with $\tau_{9.7\,\mu m} \geq 5$ but unreasonably excessive flux in the far infrared was unavoidable (Suh, 1988). After doing hundreds of calculations with various βs and other parameters we find that $\beta = 2$, i.e., $\rho(r) \propto r^{-2}$ fits observations best using properly chosen opacity pattern as discussed in the last section and other parameters.

Either a radiation pressure model (Kwok, 1975; Kozasa *et al.*, 1984) or a pulsation-shock model (Bowen, 1988) for the stellar winds predicts overall constant outflow. The results show that dust grains are accelerated relatively fast and approach and maintain terminal velocity within 3–5 R_c. Therefore, they predict overall constant outflow velocity, namely, overall density distribution should be $\rho(r) \propto r^{-2}$. Suh *et al.* (1990) finds that the change of dust density distribution for small inner portion ($r \leq 5\,R_c$) does not make much differences in emergent spectra. Therefore, we assume that the density distribution is $\rho(r) \propto r^{-2}$ throughout this work.

Figure 5 shows the results of model calculations for typical M-type Miras. The scale of λF_λ is arbitrary. The input parameters are:

dust parameters: τ (at $\lambda = 9.7$ μm) = 0.02, 0.25, 1;

stellar parameters: $T_* = 3000$ K, $L_* = 1 \times 10^4\,L_\odot$.

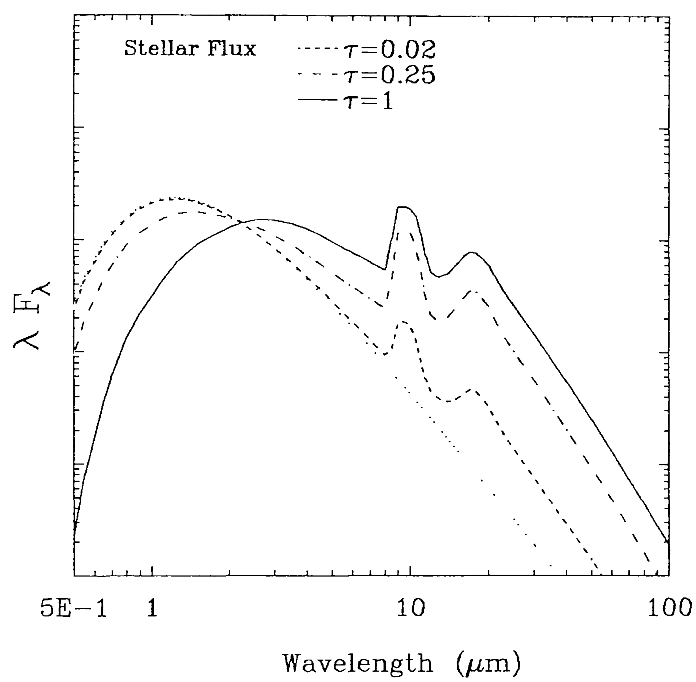

Fig. 5. The results of model calculations for M-type Miras with various optical depths at $\lambda = 9.7$ μm.

The height of emission features at 9.7 μm and 18 μm are compared with observations. The value of $(\lambda F_\lambda)_{9.7\,\mu m}/(\lambda F_\lambda)_{18\,\mu m}$ is about 4.2 (for $\tau_{9.7\,\mu m} = 0.02$) to 3.5 (for

$\tau_{9.7\ \mu m} = 0.25$). The typical observed values for Miras which show 9.7 μm and 18 μm emitting features range from 5.8–3.5 (e.g., Bedijin, 1987). When we use the opacity pattern chosen for OH/IR stars, the calculated value is from 3.5 (for $\tau_{9.7\ \mu m} = 0.02$) to 2.8 (for $\tau_{9.7\ \mu m} = 0.25$) which is about 17–20% less than for the case of Miras. So we need small value of $Q_{ext}(18\ \mu m)/Q_{ext}(9.7\ \mu m)$ for Miras; it should be around 0.5 rather than 0.7 which is for OH/IR stars.

Figure 6 shows the results of model calculations for dust thick OH/IR stars. The scale of λF_λ is arbitrary. The input parameters are:

dust parameters: τ (at $\lambda = 9.7\ \mu m$) = 15, 27, 35 ;

stellar parameters: $T_* = 2200$ K , $L_* = 1 \times 10^4 L_\odot$.

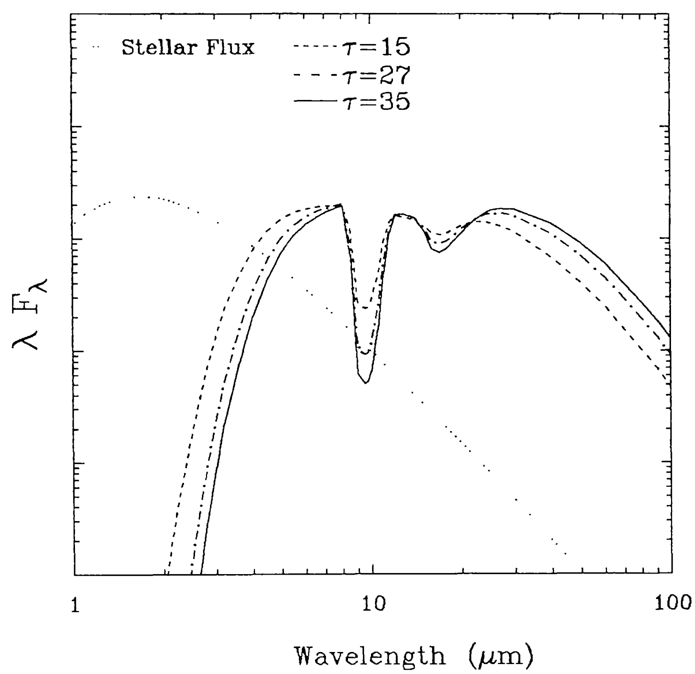

Fig. 6. The results of model calculations for OH/IR stars with various optical depths at $\lambda = 9.7\ \mu m$.

The results show clear 18 μm absorption feature. Volk and Kwok (1988) could not reproduce the 18 μm feature reasonably because they used an unsuitable opacity pattern. We find that our results closely resemble to typical observations (Herman *et al.*, 1984; Engels *et al.*, 1983) and we will closely examine the fitting with observations for typical OH/IR stars.

Figure 7 shows the dust temperature distribution for various optical depths ($\tau_{9.7\ \mu m} = 0.02$ for Miras, and $\tau_{9.7\ \mu m} = 8$, 35 for OH/IR stars). Note that the dust temperature drops below 200 K by 10 R_*, well before optical depth unity to the outer edge of the shell is reached at 18 μm for typical OH/IR stars. This suggests that an improved fit can be obtained if the temperature dependence of the opacity is explicitly

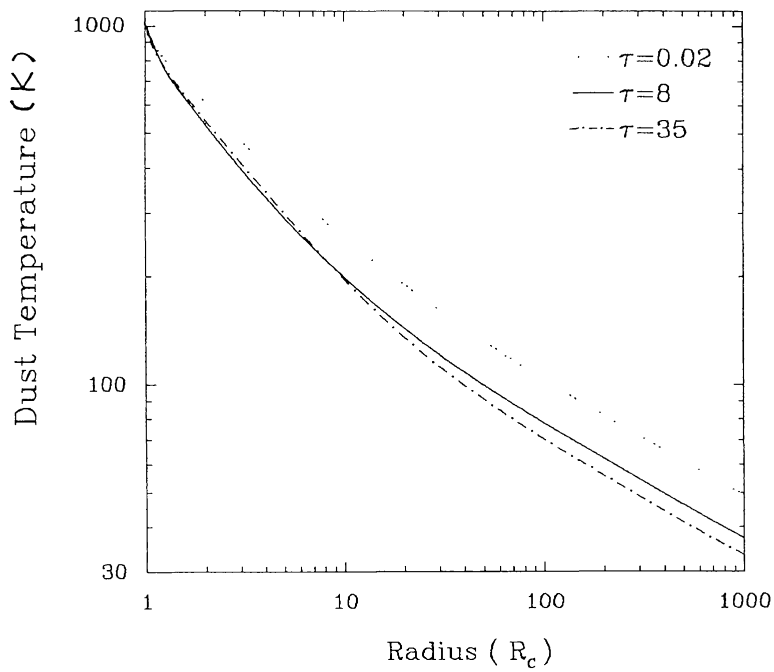

Fig. 7. Dust temperature distribution for various optical depths at $\lambda = 9.7\ \mu m$.

taken into account, rather than setting the dust absorption coefficients the same everywhere in the shell especially for OH/IR stars.

Figure 8 shows the results of calculations for OH 39.7 + 1.5 superimposed on observational data (filled triangles: Merrill and Stein, 1976; open diamond: Herman *et al.*,

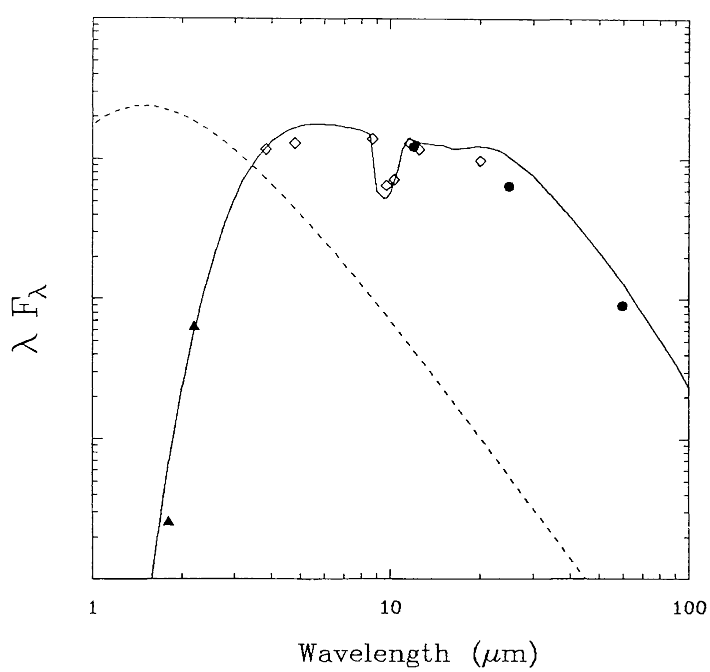

Fig. 8. The result of model calculation (solid line) superimposed on the observational data for OH 39.7 + 1.5 (symbols).

1984; filled circles: IRAS, 1986). The scale of λF_λ is arbitrarily chosen to be compared with observations. The input parameters are:

dust parameters: τ (at λ = 9.7 μm) = 8 ,

stellar parameters: $T_* = 2500$ K , $L_* = 1 \times 10^4 L_\odot$.

Figure 9 shows the results of the model calculations at three pulsation phases (3 lines) superimposed on observational data (symbols) for OH 26.5 + 0.6. Table II lists the

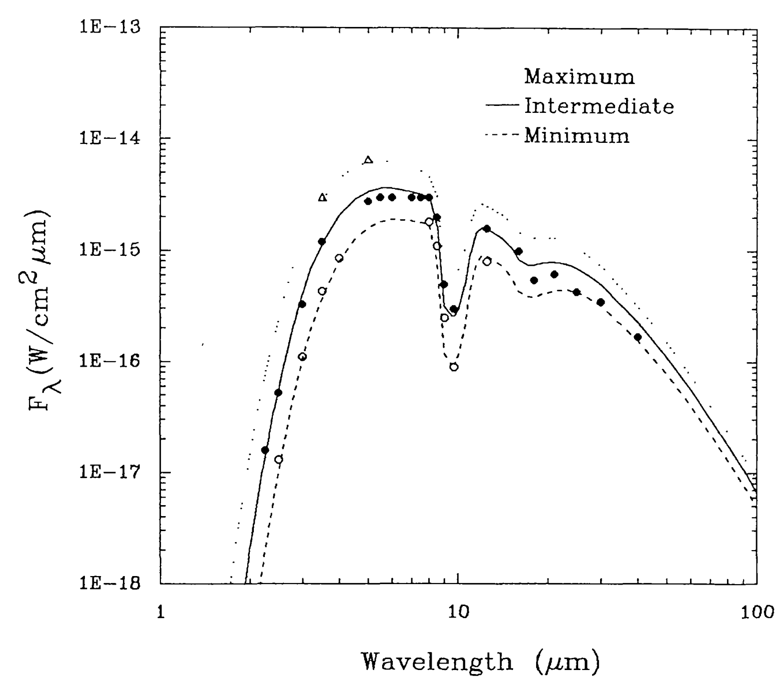

Fig. 9. The results of model calculations for OH 26.5 + 0.6 at 3 phases of pulsation (3 lines) superimposed on observational data at three phases (symbols).

TABLE II

Adopted parameters for OH 26.5 + 0.6 depending on the phase of pulsation

Parameter	Pulsation cycle phase		
	Minimum	Intermediate	Maximum
L_* ($L_\odot$)	1×10^4	1.8×10^4	3×10^4
T_* (K)	2000	2200	2400
R_* ($R_\odot$)	846	938	1017
R_c ($R_\odot$)	5100	6650	8645
τ (λ = 9.7 μm)	22	16.3	13

input model parameters. Observational data for minimum (open circles) and intermediate (filled circles) phases are from Forrest *et al.* (1978) and for maximum phase (open triangles) from the light curves of Suh (1988) and Kleinmann *et al.* (1981). Our opacity pattern deduced for OH/IR stars fits observations fairly well. Thus, a simple change in the dust condensation radius with change in stellar luminosity is adequate to explain the spectrum of OH 26.5 + 0.6 at all phases including the change of the 9.7 μm absorption depth. Suh *et al.* (1990) modeled the dust shell around OH 26.5 + 0.6 in detail depending on the phase of pulsation incorporating the results of pulsation-shock model calculations by Bowen for the object (see Bowen, 1988, for outline of his pulsation-shock model). Ideally, we may use the temperature-dependent opacity pattern

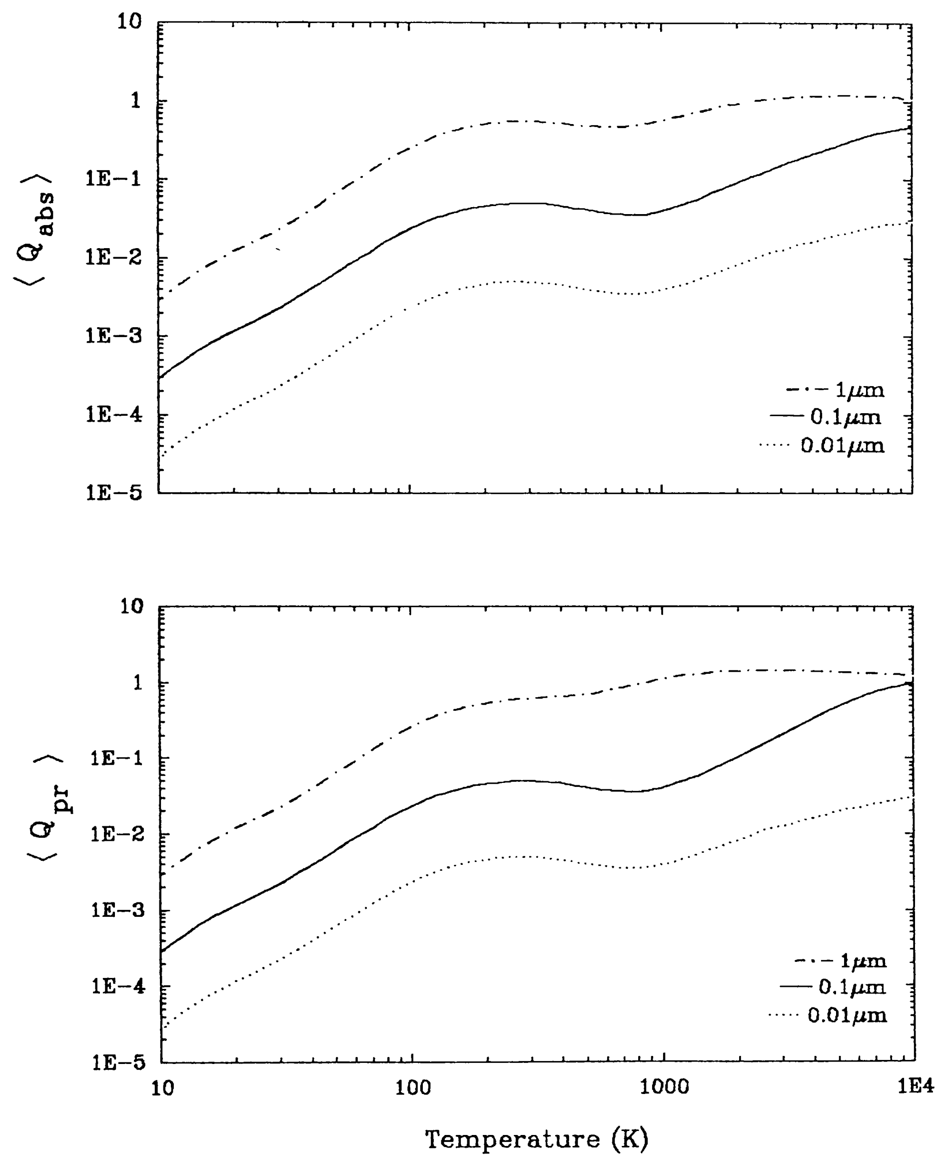

Fig. 10. Planck mean factors for various grain sizes. The optical constants deduced for OH/IR stars are used.

in model calculation which is beyond the scope of this work. That could significantly improve the fitting especially in the far-infrared.

4. Planck Mean Factors

The analysis of dust grains in the circumstellar envelope requires a knowledge of the Planck mean absorption cross-section of the grians for estimating the grian temperature, and of the Planck mean radiation pressure cross-section of the grains for estimating the dynamical effects of the grains. The Planck mean values are important for making a new pulsation-shock model which includes the dynamics of dust (e.g., Bowen, 1988).

Planck mean of some function $X(a, \lambda)$ is given by

$$\langle X(a, T)\rangle \equiv 15\left(\frac{hc}{\pi kT}\right)^4 \int_0^\infty X(a, \lambda)\lambda^{-5}\left[\exp\left(\frac{hc}{\lambda kT}\right) - 1\right]^{-1} d\lambda\,,$$

where T is the temperature. Figure 10 shows the result for various grain sizes. Our result is qualitatively similar to Gilman's (1974) result, but values are significantly different at low temperatures. At lower temperatures, our $Q_{\rm abs}$ and Q_{pr} are larger than Gilman's. That is because we used the optical constants which includes the substantial absorption in the far infrared. But at higher temperatures they are not very different.

5. Discussion

In this paper we have presented the possible opacity patterns for OH/IR stars and Miras. We cannot judge whether the difference is due to different grain material (e.g., amorphous grains) or temperature effect of the same grain material confidently. If the opacity is temperature-dependent, different opacity patterns should be used depending on the temperature of the dust grains in the shell. So it could be meaningless to define the opacity patterns for one object and another. If we assume that as Miras evolve up to dust-thick OH/IR stars the same dust grain material in the outer shell is just adding up, the grain material should show the temperature effect of opacity without changing its basic structure. Blanco *et al.* (1988) have found the similar temperature effect of opacity for hydrogenated amorphous carbon and polycyclic aromatic hydrocarbon molecules.

The experimental data are lacking, though it gives the important clue that opacity is dependent on temperature. Ideally we could use temperature-dependent opacity in radiative transfer calculations. That would give an crucial clue to solve the present problem. We expect more experiments to clarify the temperature effect of grain properties. We plan to develop the radiative transfer calculation routine that is properly dealing with the temperature effect of grain opacity.

References

Bedijin, P. J.: 1987, *Astron. Astrophys.* **186**, 136.

Blanco, A., Bussoletti, E., Colangeli, L., Fonti, S., and Orofino, V.: 1988, in E. Bussoletti, C. Fusco, and G. Longo (eds.), *Experiments on Cosmic Dust Analogues*, Kluwer Academic Publishers, Dordrecht, Holland, p. 137.

Bohren, C. F. and Huffman, D. R.: 1983, *Absorption and Scattering of Light by Small Particles*, Wiley and Sons, New York.

Bowen, G. H.: 1988, *Astrophys. J.* **329**, 299.

Day, K. L.: 1976a, *Astrophys. J.* **203**, L99.

Day, K. L.: 1976b, *Astrophys. J.* **210**, 614.

Day, K. L.: 1979, *Astrophys. J.* **234**, 158.

Day, K. L.: 1981, *Astrophys. J.* **246**, 110.

Deguchi, S.: 1980, *Astrophys. J.* **236**, 567.

Draine, B. T. and Lee, H. M.: 1984, *Astrophys. J.* **285**, 89.

Egan, M. P., Leung, C. M., and Spagna, G. F.: 1987, 'CSDUST3: A Radiation Transport Code for a Dusty Medium with 1-D Planar, Spherical or Cylindrical Geometry', preprint.

Engels, D., Kreysa, E., Schultz, G. V., and Sherwood, W. A.: 1983, *Astron. Astrophys.* **124**, 123.

Forrest, W. J., Gillet, F. C., Houck, J. R., McCarthy, J. F., Merrill, K. M., Pipher, J. L., Puetter, R. C., Russel, R. W., Soifer, B. T., and Willner, S. P.: 1978, *Astrophys. J.* **219**, 114.

Gilman, R. C.: 1974, *Astrophys. J. Suppl.* **28**, 397.

Herman, J., Isaacman, R., Sargent, A., and Habing, H. J.: 1984, *Astron. Astrophys.* **139**, 171.

IRAS Catalogues and Atlases: 1986, *Point Source Catalogue,* US Government Publication Office.

Jones, T. W. and Merrill, K. M.: 1976, *Astrophys. J.* **209**, 509.

Kleinmann, S. G., Gillet, F. C., and Joyce, R. R.: 1981, *Ann. Rev. Astron. Astrophys.* **19**, 411.

Kozasa, T., Hasegawa, H., and Seki, J.: 1984, *Astrophys. Space Sci.* **98**, 61.

Kwok, S.: 1975, *Astrophys. J.* **198**, 583.

Leung, C. M.: 1976, *J. Quant. Spectr. Rad. Trans.* **16**, 559.

Merrill, K. M. and Stein, W. A.: 1976, *Publ. Astron. Soc. Pacific* **88**, 285.

Papoular, R. and Pégourié, B.: 1986, *Astron. Astrophys.* **156**, 199.

Prégourié, B. and Papoular, R.: 1985, *Astron. Astrophys.* **142**, 451.

Suh, K.-W.: 1988, Ph.D. Thesis, University of Minnesota, Minneapolis.

Suh, K.-W., Jones, T. J., and Bowen, G. H.: 1990, *Astrophys. J.* **358**, 588.

Treffers, R. and Cohen, M.: 1974, *Astrophys. J.* **188**, 545.

Volk, K. and Kwok, S.: 1988, *Astrophys. J.* **331**, 435.

Werner, M. W., Beckwith, S., Gatley, I., Sellgren, K., Berriman, G., and Whiting, D. L.: 1980, *Astrophys. J.* **239**, 540.

Woolf, N. J. and Ney, E. P.: 1969, *Astrophys. J.* **155**, 181.

Yamamoto, T. and Hasegawa, H.: 1977, *Prog. Theor. Phys.* **58**, 816.